DOI: 10.1002/asia.201000651

Gold(I)-Catalyzed Enantioselective Intermolecular Hydroarylation of Allenes with Indoles and Reaction Mechanism by Density Functional Theory Calculations

Ming-Zhong Wang,[a] Cong-Ying Zhou,[a] Zhen Guo,[a] Ella Lai-Ming Wong,[a] Man-Kin Wong,[a, b] and Chi-Ming Che*[a]

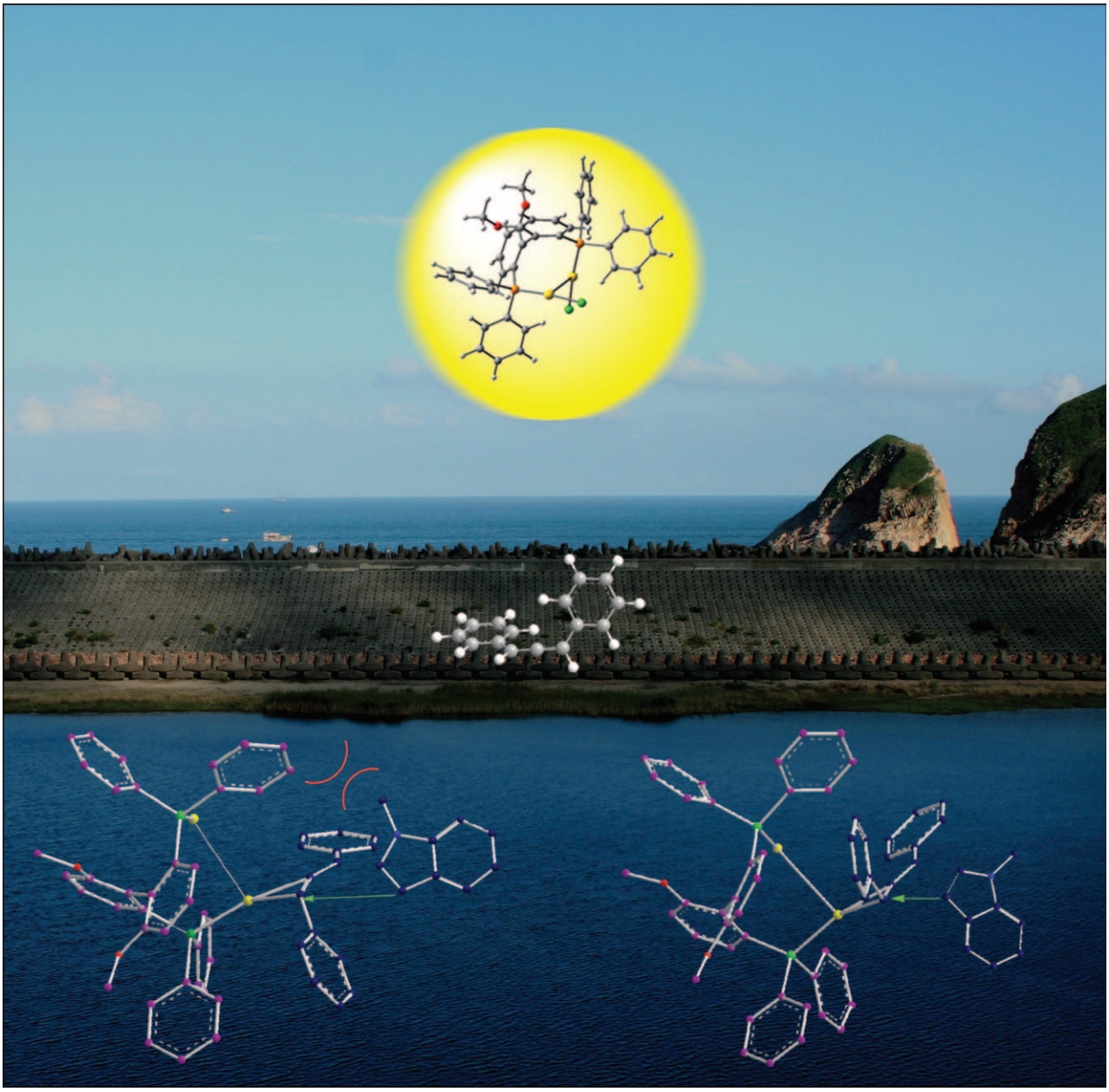

Abstract: Chiral binuclear gold(I) phosphine complexes catalyze enantioselective intermolecular hydroarylation of allenes with indoles in high product yields (up to 90%) and with moderate enantioselectivities (up to 63% *ee*). Among the gold(I) complexes examined, better *ee* values were obtained with binuclear gold(I) complexes, which displayed intramolecular Au^I–Au^I interactions. The binuclear gold(I) complex **4c** [$(AuCl)_2$(**L3**)] with chiral biaryl phosphine ligand (*S*)-(−)-MeO-biphep (**L3**) is the most efficient catalyst and gives the best *ee* value of up to 63%. Substituents on the allene reactants have a slight effect on the enantioselectivity of the reaction. Electron-withdrawing groups on the indole substrates decrease the enantioselectivity of the reaction. The relative reaction rates of the hydroarylation of 4-X-substituted 1,3-diarylallenes with *N*-methylindole in the presence of catalyst **4c** [$(AuCl)_2$(**L3**)]/AgOTf [**L3** = (*S*)-(−)-MeO-biphep], determined through competition experiments, correlate ($r^2 = 0.996$) with the substituent constants σ. The slope value is −2.30, revealing both the build-up of positive charge at the allene and electrophilic nature of the reactive Au^I species. Two plausible reaction pathways were investigated by density functional theory calculations, one pathway involving intermolecular nucleophilic addition of free indole to aurated allene intermediate and another pathway involving intramolecular nucleophilic addition of aurated indole to allene via diaurated intermediate **E2**. Calculated results revealed that the reaction likely proceeds via the first pathway with a lower activation energy. The role of Au^I–Au^I interactions in affecting the enantioselectivity is discussed.

Keywords: allenes · enantioselectivity · gold · hydroarylation · indoles

Introduction

Stereoselective addition of indolyl C–H bonds across C–C multiple bonds is an efficient and atom-economical strategy for the synthesis of enantiopure indole compounds which are prevalent in bioactive natural products and drug leads.[1] It has been reported that chiral Lewis acids and Brønsted acids can catalyze asymmetric Friedel–Crafts alkylation of indole with an alkene conjugated to an electron-withdrawing group (ketone or nitro group) in high enantioselectivity.[2] This strategy involves the interaction of a chiral Lewis acid or Brønsted acid with an electron-withdrawing substituent on the alkene. However, the catalytic enantioselective hydroarylation of unactivated C–C multiple bonds with indoles through direct coordination and activation of π bonds by transition-metal ions remains a formidable challenge.[3]

In recent years, Au^I and Au^{III} complexes have emerged to become useful catalysts for electrophilic activation of C–C multiple bonds toward nucleophilic attack.[4] Although Au^I complexes can efficiently and selectively catalyze a number of organic transformations under mild conditions, only a handful of examples of Au^I-catalyzed enantioselective organic transformations have been reported.[5,6] Among them, a notable example is enantioselective intramolecular functionalization or isomerization of allenes catalyzed by chiral binuclear gold(I) phosphine complexes [$(AuX)_2$(P-P)] (P-P = chiral bisphosphine) with high enantioselectivity.[6] In early 2007, the groups of Toste and Widenhoefer independently reported the gold(I)-catalyzed enantioselective intramolecular hydroalkoxylation[6a] and hydroamination[6b] reactions of allenes with up to 99% enantioselectivity. Shortly after, Widenhoefer and co-workers extended this protocol to enantioselective intramolecular hydroarylation of 2-(allenyl)indoles (72–92% *ee*).[3d] With a similar catalytic system, Toste and co-workers developed a highly enantioselective intramolecular [2+2] cycloaddition of γ-eneallenes (54–97% *ee*).[6c] In the same year, Gagné and co-workers reported a gold(I)-catalyzed enantioselective hydrovinylation of allenes to form substituted vinylcyclohexenes (45–72% *ee*).[6d] More recently, López and co-workers reported an enantioselective [4+2] intramolecular cycloaddition of allenedienes catalyzed by chiral gold(I) phosphoramidite complexes (52–97% *ee*).[6h] Despite these advances, to our knowledge, there has been no report on gold-catalyzed enantioselective intermolecular hydroarylation of allenes with arenes.[7] As part of our program to develop gold-catalyzed functionalization of C–C multiple bonds,[8] herein is described an efficient enantioselective intermolecular hydroarylation of racemic allenes with indoles catalyzed by chiral binuclear gold(I) phosphine complexes. Our DFT calculations revealed that the reaction mechanism involves intermolecular nucleophilic addition of free indole to an aurated allene intermediate, and the intramolecular Au^I–Au^I interaction plays a key role in affecting the enantioselectivity of the reaction.

[a] M.-Z. Wang, Dr. C.-Y. Zhou, Dr. Z. Guo, Dr. E. L.-M. Wong, Dr. M.-K. Wong, Prof. C.-M. Che
Department of Chemistry, State Key Laboratory of Synthetic Chemistry, and Open Laboratory of Chemical Biology of the Institute of Molecular Technology for Drug Discovery and Synthesis
The University of Hong Kong
Pokfulam Road, Hong Kong (P. R. China)
Fax: (+852) 2857-1586
E-mail: cmche@hku.hk

[b] Dr. M.-K. Wong
Department of Applied Biology and Chemical Technology
The Hong Kong Polytechnic University
Hung Hom, Kowloon, Hong Kong (P. R. China)

Supporting information for this article is available on the WWW under http://dx.doi.org/10.1002/asia.201000651.

Results and Discussion

We recently reported a gold- and a silver-mediated highly enantioselective synthesis of axially chiral allenes.[9] At the outset, we investigated the enantioselective hydroarylation

of chiral allenes with indoles. The reaction of chiral allene **2a** (98% *ee*) with *N*-methyl indole **1a** in the presence of 5 mol% AuCl/AgOTf at room temperature for 6 h led to 3-alkylated indole **3a** in 95% yield of isolated product without any enantioselectivity being observed (Table 1, entry 1). A

Table 1. Gold-catalyzed intermolecular hydroarylation of axially chiral allene **2a** with indole **1a**.[a]

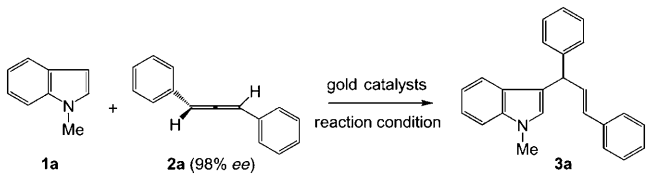

Entry	Catalyst	Solvent	*t* [h]	Yield [%][b]	*ee* [%][c]
1	AuCl/AgOTf	THF	6	95	0
2	(PPh_3)AuCl/AgOTf	toluene	6	90	5
3	(PPh_3)AuCl/AgOTf	THF	6	92	0
4	[P(*t*Bu)$_2$(*o*-biphenyl)]AuCl/AgOTf	toluene	6	60	0
5	[P(4-MeOC$_6$H$_4$)$_3$]AuCl/AgOTf	toluene	12	85	0
6	(PEt_3)AuCl/AgOTf	toluene	12	83	0
7	$AuCl_3$	toluene	12	trace	–
8	$AuCl_3$/AgOTf	toluene	6	trace	–
9	30 mol% AgOTf	toluene	12	trace	–

[a] Reactions were conducted with 0.6 mmol of **1a**, 0.3 mmol of **2a**, and 5 mol% catalyst at room temperature. [b] Yield of isolated product. [c] *ee* values were determined by chiral column.

Table 2. Screening of ligands and reaction conditions for enantioselective intermolecular hydroarylation of racemic allene **2b** with indole **1a**.[a]

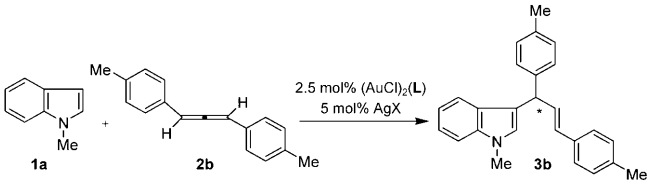

Entry	Catalyst	Solvent	*t* [h]	Yield [%][b]	*ee* [%][c]
1	(**4a**)	toluene	12	91	18
2	(**4b**)	toluene	12	85	18
3	(**4c**)	toluene	16	90	60
4	(**4d**)	toluene	36	52	17
5	(**4e**)	toluene	16	90	50
6	(**4f**)	toluene	16	82	6.5
7	(**4g**)	toluene	16	89	25
8	(**4h**)	toluene	16	57	49
9[d]	$PtCl_2$(**L3**) (**4i**)	toluene	16	trace	–
10[d]	$PtCl_2$(**L4**) (**4j**)	toluene	16	trace	–
11	(**4c**)	THF	16	82	43
12	(**4c**)	CH_3CN	16	65	48
13	1 mol% **4c**/2 mol% AgOTf	toluene	16	32	53
14	5 mol% **4c**/10 mol% AgOTf	toluene	16	93	39
15	2.5 mol% **4c**/10 mol% AgOTf	toluene	16	87	58

[a] Reactions were conducted with 1.5 mmol of **1a**, 0.3 mmol of **2b**, and 2.5 mol% $(AuCl)_2$(**L**) /5 mol% AgOTf in 1 mL of toluene at 25°C for 16–36 h. [b] Yield of isolated product. [c] *ee* values were determined by chiral column; see the Supporting Information. [d] Reaction was conducted at 60°C for 16 h.

number of gold(I) catalysts having different phosphine ligands were screened. Although (PPh_3)AuCl/AgOTf, [P(*t*Bu)$_2$(*o*-biphenyl)]AuCl/AgOTf, [P(4-MeOC$_6$H$_4$)$_3$]AuCl/AgOTf and (PEt_3)AuCl/AgOTf all catalyzed the reaction in high product yields, racemic product was found for each of the cases examined without chirality transfer (Table 1, entries 2–5). This result is consistent with the works reported by Toste, Widenhoefer, and Krause et al. showing that axially chiral allenes could be racemized by gold complexes.[10] The other metal salts $AuCl_3$, $AuCl_3$/AgOTf, and AgOTf failed to catalyze this reaction.

As Au^I complexes with chiral biaryl phosphine ligands have been demonstrated to be excellent catalysts for enantioselective intramolecular functionalization of allenes, we investigated the reaction of racemic allenes with indoles catalyzed by this class of binuclear gold(I) complexes.[6] In preliminary experiments, treatment of racemic allene **2b** and *N*-methyl indole **1a** with a mixture of chiral gold(I) catalyst **4a** (2.5 mol%) and AgOTf (5 mol%) in toluene at room temperature for 12 h led to 3-alkylated indole **3b** in 91% isolated yield with 18% *ee* (Table 2, entry 1). Under the same conditions, a series of chiral binuclear gold(I) phosphine complexes were examined (Figure 1). Complex **4c** with (*S*)-(−)-MeO-biphep ligand was found to give the best result for intermolecular hydroarylation of **2b** with **1a**, affording product in 90% isolated yield with 60% *ee* (Table 2, entry 3). Interestingly, complex **4d**, previously reported to efficiently catalyze enantioselective transformation of allenes, displayed a low catalytic activity towards intermolecular hydroarylation of **2a** with **1a**, furnishing product in 52% isolated yield with 17% *ee* and with a long reaction time of 36 h (Table 2, entry 4). Complex **4e** with an electron-donating substituent on the phosphine ligand catalyzed the reaction with a better enantioselectivity than complex **4f** with a phosphine ligand having an electron-withdrawing substituent (Table 2, entries 5 and 6). The Pt^{II} complexes **4i** and **4j** with ligand (*S*)-(−)-MeO-biphep (**L3**) and (*S*)-3,5-*t*Bu$_2$-4-MeO-biphep (**L4**), respectively, which have been reported to be effective catalyst for enantioselective intramolecular hydroarylation of alkenes with indoles,[3c] failed to catalyze this reaction even at a temperature of up to 60°C (Table 2, entries 9 and 10). With **4c** as catalyst, the effect of solvent was examined. Both THF and acetonitrile were found to give the desired products in lower product yields and decreased enantioselectivity (Table 2, entries 11 and 12). Decreasing the temperature to 0°C led to a low substrate conversion of **2b**. We also examined the effect of catalyst loading on the enantioselective hydroarylation of **2b** with **1a** (Table 2, entries 13–15). A mixture of complex **4c** (1 mol%) and AgOTf (2 mol%) as catalyst led to hydroarylation product in 32% yield with 53% *ee* (Table 2, entry 13). Increasing the catalyst loading to 5 mol% of **4c** and 10 mol% of AgOTf resulted in a reduced enantioselectivity to 39%

CHEMISTRY
AN ASIAN JOURNAL

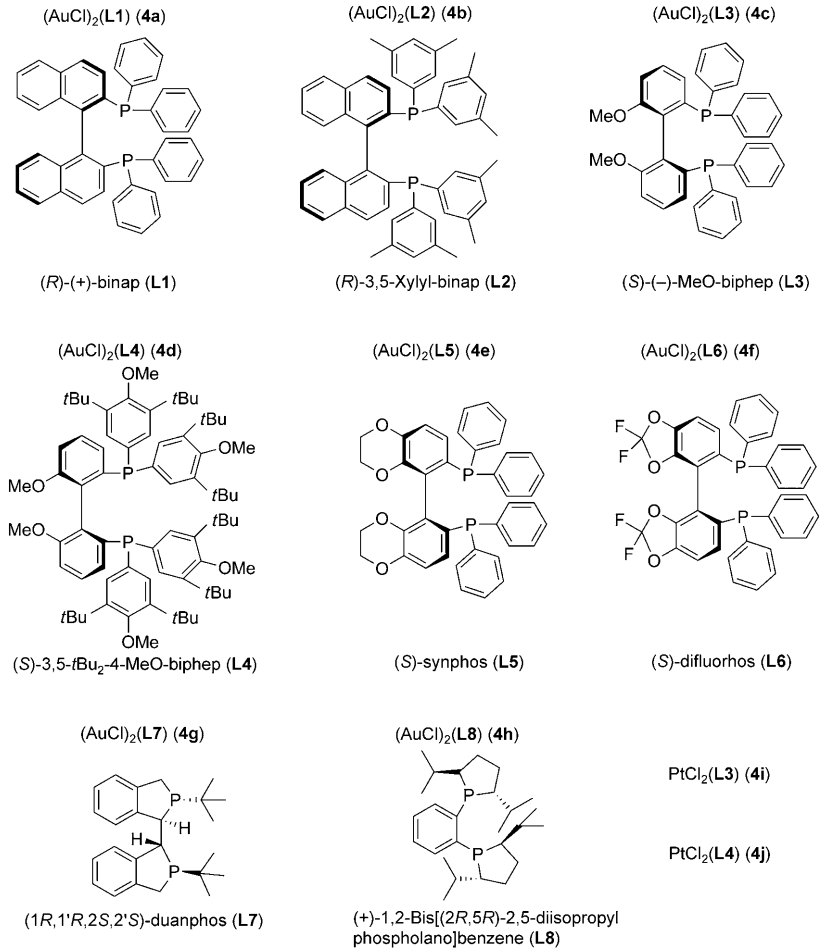

Figure 1. Chiral dimetal phosphine catalysts.

(Table 2, entry 14). The use of excess AgOTf had a slight effect on both the product yield and enantioselectivity (Table 2, entry 15). After optimization, the protocol with **4c** (2.5 mol%) and AgOTf (5 mol%) at room temperature was found to give the best result.

With the optimized conditions, we examined the scope of Au^I-catalyzed enantioselective intermolecular hydroarylation of racemic allenes with indoles (Table 3). Most of the 1,3-diaryl allenes and indoles underwent hydroarylation reaction to give the corresponding 3-alkylated indoles in good isolated yields with moderate enantioselectivities. A *para* substituent on the aryl moiety of allenes has a slight effect on both the product yield and enantioselectivity. For example, the reactions of *N*-methyl indole **1a** with racemic allenes **2b** (4-Me), **2c** (4-*t*Bu), and **2d** (4-OMe) gave the corresponding products in high yields (81–90%) with similar enantioselectivities (53–60% *ee*, Table 3, entries 2–4). Hydroarylation of racemic allene **2e** (4-F) having an electron-withdrawing substituent led to the corresponding product in a slightly higher enantioselectivity of 63% *ee* and in 72% isolated yield (Table 3, entry 5). However, the *ortho* 2-Me substituent in racemic allene **2f** resulted in low product yield and enantioselectivity (7% *ee*, Table 3, entry 6). The reactions of racemic allenes with various substituted indoles have been examined. Electron-withdrawing groups were found to decrease the reaction enantioselectivity. For example, hydroarylation of **2b** with 5-chloro-*N*-methyl indole **1b** led to the corresponding 3-alkylated indole **3g** in 40% *ee* (Table 3, entry 7); the reaction of **2b** with 6-carboxyl-*N*-methyl indole **1c** gave the product **3h** in 37% *ee* (Table 3, entry 8). The reaction of indole **1d** having a methyl group at the C-2 position with allene **2b** gave lower product yield and enantioselectivity than that of the reaction with **1a** (41% *ee*, Table 3, entry 9). *N*-Benzyl indole also led to lower enantioselectivity than **1a** (35% *ee*, Table 3, entry 10). Using allene **2e** (4-F) as a substrate, its reactions with various indole compounds gave the corresponding hydroarylation products in moderate enantioselectivities (43–51% *ee*, Table 3, entries 11–14). The **4c**-catalyzed hydroarylations of alkyl-substituted allenes with indoles were also examined. When cyclohexalallene was used, the substrate conversion was low (<5%) under the same reaction conditions.

Competitive Hydroarylation of Allenes with *N*-Methylindole

To get an insight into the reaction mechanism, the relative reaction rates of *p*-X-C_6H_4CH=C=CH(*p*-X-C_6H_4) [X=H (**2a**), Me (**2b**), OMe (**2d**), and F (**2e**)] with *N*-methylindole **1a** using **4c** as catalyst were examined by ^{1}H NMR analysis of the corresponding hydroarylation products. The results are depicted in Figure 2. The rate data display a good Hammett linear free-energy relationship ($r^2=0.996$). The slope value ρ was determined to be −2.30, similar to the value (−2.40) obtained for the reaction of 4-substituted styrene derivatives with $[(IPr)Au(NCAr_F)]^+ SbF_6^-$ [IPr=1,3-bis(2,6-diisopropylphenyl) imidazol-2-ylidene],[11] revealing the build-up of positive charge at the allene and electrophilic character of the active Au^I-allene reaction intermediate. This is consistent with the findings that allene **2d** with an electron-donating *p*-methoxy substituent is more reactive than both allenes **2a** and **2e** with H and F substituents, respectively.

Table 3. Gold(I)-catalyzed enantioselective intermolecular hydroarylation of allenes with indoles.[a]

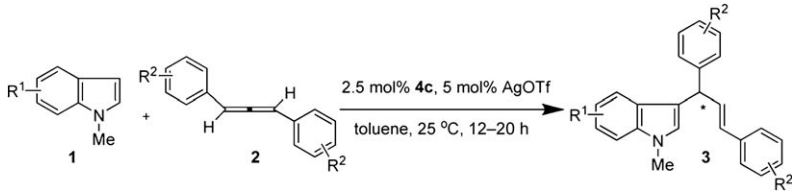

Entry	Indole	Allene	Product	Yield [%][b]	*ee* [%][c]
1	 **1a**	**2a**: R^2=H	**3a**: R^2=H	85	41
2	**1a**	**2b**: R^2=4-Me	**3b**: R^2=4-Me	90	60
3	**1a**	**2c**: R^2=4-*t*Bu	**3c**: R^2=4-*t*Bu	85	56
4	**1a**	**2d**: R^2=4-OMe	**3d**: R^2=4-OMe	81	53
5	**1a**	**2e**: R^2=4-F	**3e**: R^2=4-F	72	63
6	**1a**	**2f**: R^2=2-Me	**3f**: R^2=2-Me	38	7
7	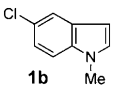 **1b**	**2b**	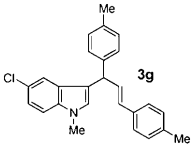 **3g**	75	40
8	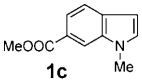 **1c**	**2b**	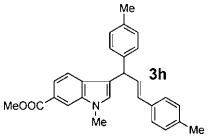 **3h**	73	37
9	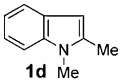 **1d**	**2b**	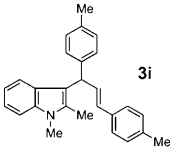 **3i**	85	41
10	 **1e**	**2b**	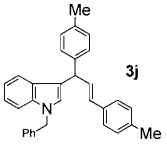 **3j**	85	35
11	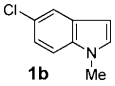 **1b**	**2e**	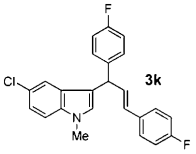 **3k**	67	51
12	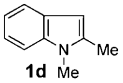 **1d**	**2e**	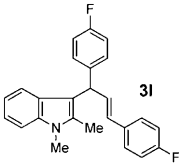 **3l**	83	45
13	 **1f**	**2e**	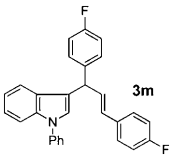 **3m**	75	43
14	 **1g**	**2e**	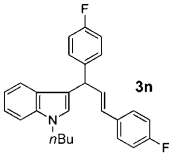 **3n**	85	47

[a] Reactions were conducted with 1.5 mmol of indole **1**, 0.3 mmol of racemic allene **2**, and 2.5 mol% **4c**/5 mol% AgOTf in 1 mL toluene for 12–20 h. [b] Yield of isolated product. [c] *ee* values were determined by chiral column; see the Supporting Information.

Deuterium-Labelling Experiment

A deuterium-labelling experiment was performed (Scheme 1). The reaction of **2b** with **1a** in D_2O/toluene led to **3o** with 68% deuterium incorporation (Scheme 1a). Treatment of 3-deuterium-*N*-methyl indole with **2b** gave **3o** with 42% deuterium incorporation (Scheme 1b). The moderate deuterium incorporation can be rationalized by the presence of trace water in the reaction mixture. All of these data reveal that the catalysis involves a crucial intermolecular hydrogen atom transfer step.

^{31}P NMR Study

A mixture of Ph_3PAuCl (1 equiv) and AgOTf (1 equiv) in $CDCl_3$ was analyzed by ^{31}P NMR, showing a peak at δ=30.8 ppm assigned to $Ph_3PAuOTf$. To this reaction mixture was added **1a** (1.1 equiv) and the mixture was stirred for 180 min at room temperature. A new peak at δ=45.10 ppm was observed in the ^{31}P NMR spectrum depicted in Figure 3. This chemical shift is similar to related values of known vinyl-Au^{I} and aryl-Au^{I} phosphine complexes (at around 44 ppm),[12] suggesting a C−Au bond formation between the indole and gold(I) complex. Similarly, the ^{31}P NMR spectrum of a solution mixture containing complex **4c** (1 equiv), AgOTf (2 equiv), and indole **1a** (1 equiv) for a reaction time of 180 min in $CDCl_3$ also gave a signal peak at δ=43.8 ppm (Figure 4), which is characteristics of aryl-Au^{I} phosphine complexes.

X-ray Crystal Structures

The structures of the complexes **4c** [$(AuCl)_2$(**L3**)], **4f**

CHEMISTRY
AN ASIAN JOURNAL

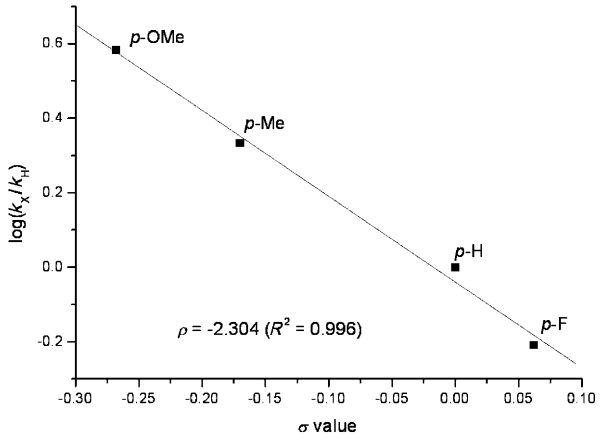

Figure 2. Hammett plot derived for the hydroarylation of allenes with indole **1a** catalyzed by **4c** (2.5 mol%) and AgOTf (5 mol%).

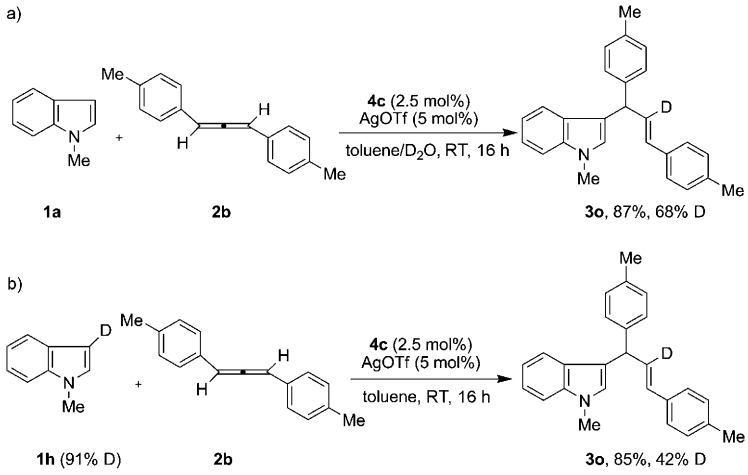

Scheme 1. Deuterium-labelling experiment.

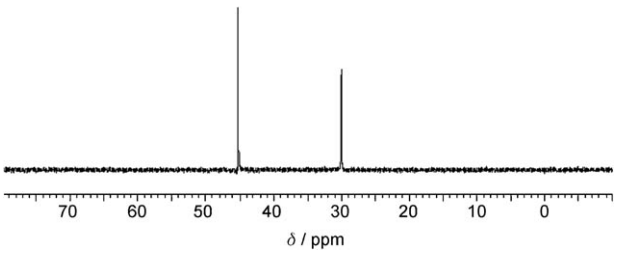

Figure 3. ^{31}P NMR spectrum of the reaction mixture by reacting $(PPh_3)AuCl$/AgOTf (1:1) with *N*-methylindole **1a** in $CDCl_3$ for 180 min.

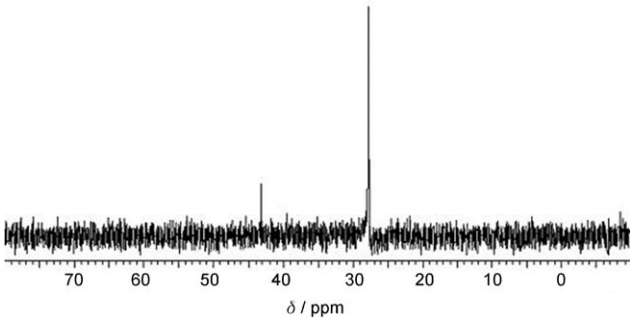

Figure 4. ^{31}P NMR spectrum of the reaction mixture by reacting **4c**/AgOTf (1:2) with *N*-methylindole **1a** in $CDCl_3$ for 180 min.

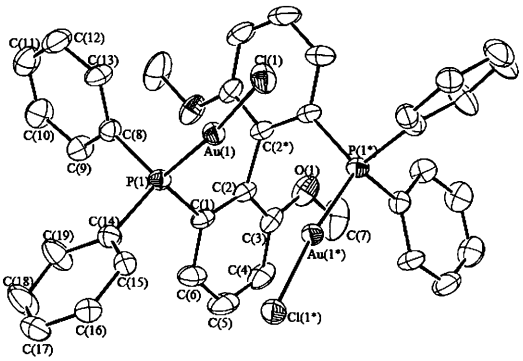

Figure 5. X-ray crystal structure of complex **4c** (thermal ellipsoids probability: 30%); for clarity, hydrogen atoms and solvent molecules are not shown. Selected bond lengths [Å] and angles [°]: Au(1)-Au(1*) 3.1473(5), Au(1)-P(1) 2.2415(14), Au(1)-Cl(1) 2.2932(15); P(1)-Au(1)-Cl(1) 173.69(5), P(1)-Au(1)-Au(1*) 187.32(4), Cl(1)-Au(1)-Au(1*) 198.33(4).

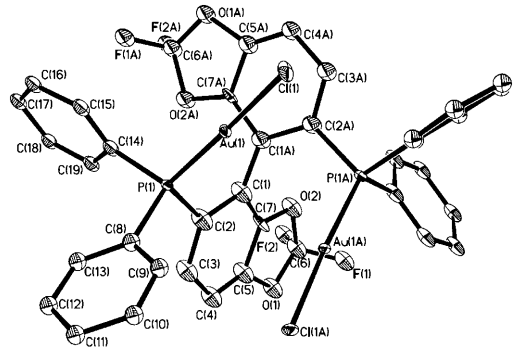

Figure 6. X-ray crystal structure of complex **4f** (thermal ellipsoids probability: 30%); for clarity, hydrogen atoms and solvent molecules are not shown. Selected bond lengths [Å] and angles [°]: Au(1)-Au(1A) 3.786, Au(1)-P(1) 2.231(3), Au(1)-Cl(1) 2.289(4); P(1)-Au(1)-Cl(1) 176.41(14), P(1A)-Au(1A)-Cl(1A) 176.41(14), C(8)-P(1)-Au(1) 111.6(5).

[$(AuCl)_2$(**L6**)], **4d** [$(AuCl)_2$(**L4**)],[13,18] and **4h** [$(AuCl)_2$(**L8**)] were determined by X-ray crystallography and are shown in Figures 5–7.[13] The crystals were grown by slow diffusion of hexane into dichloromethane solutions. As shown in Figures 5 and 7, the intramolecular Au–Au distances are 3.1473(5) Å for **4c** and 2.9347(3) Å for **4h**, respectively, indicating the presence of intramolecular Au–Au interaction. This interaction can render the catalyst less flexible. No intramolecular Au–Au interaction was observed in **4f** (3.786 Å, Figure 6).

DFT Calculations

Recently, gold(I)-catalyzed functionalization and isomerization of unsaturated C–C bonds have been attracting a surge

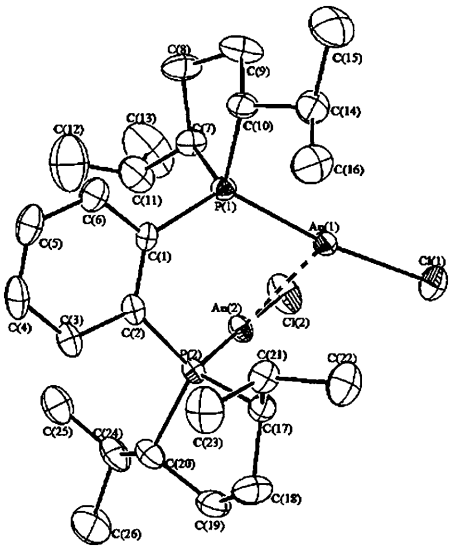

Figure 7. X-ray crystal structure of complex **4h** (thermal ellipsoids probability: 30%); for clarity, hydrogen atoms and solvent molecules are not shown. Selected bond lengths [Å] and angles [°]: Au(1)-Au(2) 2.9347(3), Au(1)-P(1) 2.2444(12), Au(1)-Cl(1) 2.2842(15); P(1)-Au(1)-Cl(1) 172.09(6), P(1)-Au(1)-Au(2), 85.60 (3), Cl(1)-Au(1)-Au(2), 100.59 (5).

of interest. In many cases, the catalysis involves a reactive monoaurated intermediate such as a gold–π complex, vinyl–gold complex, or gold–carbene species. In 2008, Toste and co-workers postulated the involvement of a diaurated intermediate in the gold-catalyzed cycloisomerization of 1,5-allenynes on the basis of density functional theory (DFT) calculations. The diaurated intermediate was proposed to be a *gem*-diauraalkene complex in a three-center two-electron mode.[14] Subsequently Gagné et al. provided experimental support for a diaurated reaction intermediate involved in Au^I-catalyzed intramolecular hydroarylation of allenes,[15] the structure of which is similar to the intermediate proposed by Toste. More recently, Bandini and co-workers reported an enantioselective intramolecular binuclear gold(I) complex catalyzed allylic alkylation of indole with allylic alcohol, presumably via a diaurated reaction intermediate with dual activation of the C=C bond and hydroxy group.[3g] In this work, the formation of an aryl-Au^I phosphine complex was observed by analysis of the ^{31}P NMR spectrum of the reaction mixture obtained by reacting complex **4c**/AgOTf and indole **1a** in $CDCl_3$ for 180 min. To get insight into the reaction mechanism, two plausible reaction pathways were investigated by density functional theory calculations: 1) the pathway involving intermolecular nucleophilic addition of free indole to aurated allene intermediate **E1** (Scheme 2); 2) the pathway involving intramolecular nucleophilic addition of aurated indole to allene via diaurated intermediate **E2** in which two gold(I) atoms simultaneously bind to allene and indole.

A computational study using DFT (B3LYP/6–31G*, Lanl2dz for Au) was undertaken to model the digold(I) phosphine complex catalyzed hydroarylation of allene with indole. In order to reduce the computational time, the

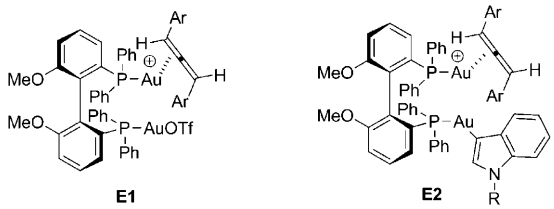

Scheme 2. Proposed reaction intermediates.

phenyl groups of the digold(I) phosphine complex, $[(\mathbf{L3})Au_2]^{2+}$ (**L3** = MeO-biphep)], were replaced by methyl groups. This leads to the model complex $[(\mathbf{L})Au_2]^{2+}$ (**L** = MeO-bimep)] employed in our calculation. The calculated free energies are depicted in Figure 8 and Figure 9. The optimized stationary structures (minima, saddle points) on the potential energy surface of reactions, energies, and selected key geometry parameters are depicted in the Supporting Information.

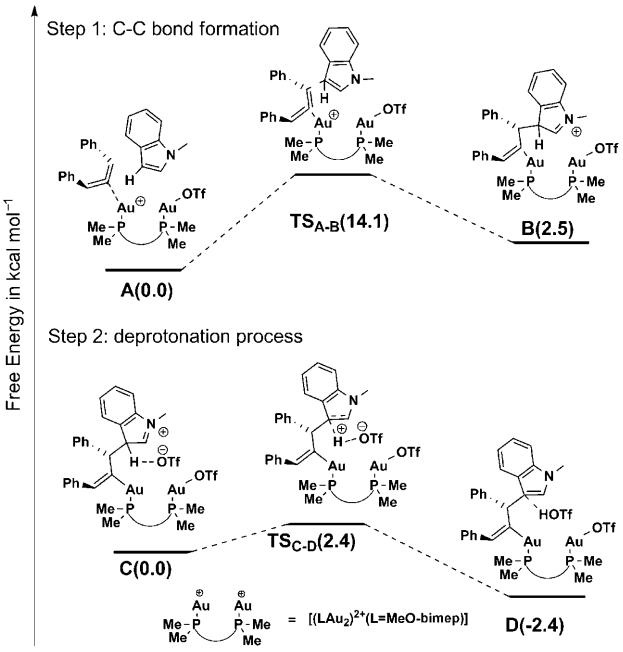

Figure 8. Calculated free energies for intermolecular reaction of allene with indole via monoaurated intermediate using DFT approach (B3LYP/6-31G*, Lanl2dz for Au).

With the optimized geommetry as depicted in Figure 8, the first reaction pathway starts with intermediate **A** composed of indole and a gold(I)-allene complex in which one gold(I) center coordinates to allene and the other binds to triflate. The coordination of the gold(I) complex to allene is supported by the Hammett plot experiment with a ρ value of −2.30, revealing the build-up of positive charge at the allene. The calculation showed that the nucleophillic addition of indole to gold(I)-activated allene is relatively facile, requiring an activation free energy of 14.1 kcal mol^{-1} via transition state $\mathbf{TS_{A\text{-}B}}$. Formation of complex **B** is endergonic

CHEMISTRY
AN ASIAN JOURNAL

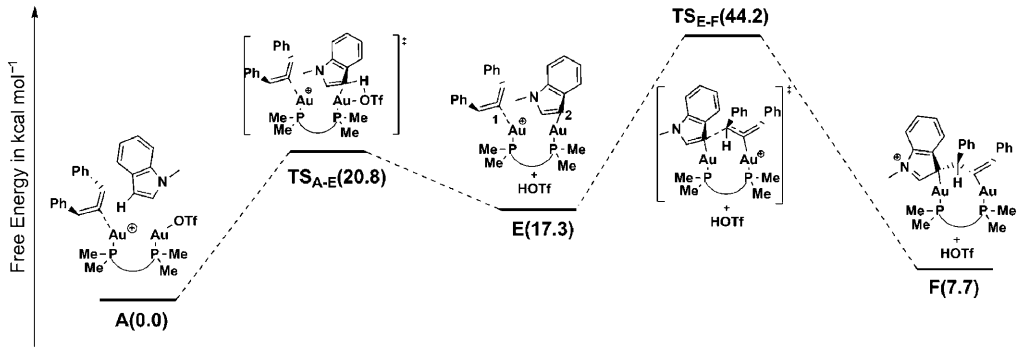

Figure 9. Calculated free energies for the hydroarylation reaction via intermediate **E** by DFT calculation (B3LYP/6-31G*, Lanl2dz for Au).

by 2.5 kcal mol^{-1}. This step leads to C–C bond formation between allene and indole. The subsequent step is rearomatization from intermediate **C** to **D** through a deprotonation process assisted by triflate anion. The transition state **TS$_{C-D}$** for this step needs a low activation energy of 2.4 kcal mol^{-1}. Finally, intermediate **D** undergoes demetalation to yield hydroarylation product and regenerate the gold(I) catalyst. The relative low reaction barrier from intermediate **A** to **D** reveals that the commonly accepted mechanism involving a monoaurated intermediate is operative in this dinuclear gold(I) phosphine complex catalyzed hydroarylation of allene with indole.

The potential free energy surface for the second pathway is shown in Figure 9. With triflate-assisted deprotonation,[16] the binuclear gold(I) phosphine complex [(Au$_2$(**L**)(allene)-(OTf)]$^+$ interacts with the indole to generate the digold(I) species [(Au$_2$(**L**)(allene)-(indole–H)]$^+$ **E** via transition state **TS$_{A-E}$**. The transition state **TS$_{A-E}$** has an activation energy barrier of 20.8 kcal mol^{-1} in the gas phase. The intermediate **E** formed via **TS$_{A-E}$** is more unstable than **A** by 17.3 kcal mol^{-1}. However, the second step of C–C bond formation between gold-activated allene and aurated indole via **TS$_{E-F}$** requires another activation energy of 26.9 kcal mol^{-1} from **E** to **F**. Thus, the total reaction barrier from intermediate **A** to **F** is 44.2 kcal mol^{-1} in the gas phase, revealing that the hydroarylation via diaurated species **E** is unfavorable. As a result, the reaction more likely proceeds via the first pathway owing to a relatively low reaction barrier.

Proposed Reaction Mechanism

According to the above experimental results and computational study, a plausible reaction mechanism is depicted in Scheme 3. The cationic gold(I) coordinates to the allene to give intermediate **I** and the coordination facilitates nucleophilic attack of the allene by free indole to generate intermediate **II**. Subsequent protonolysis of intermediate **II** affords the desired product and regenerates the catalyst.

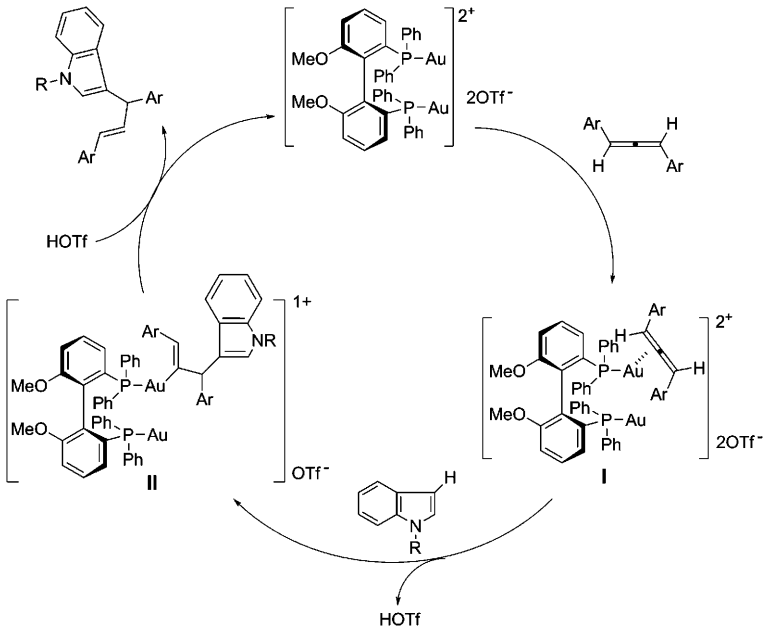

Scheme 3. Proposed reaction pathway.

Stereoselectivity

As depicted in Scheme 4a,b, the coordination of gold complex to racemic allene gives four isomeric gold-allene intermediates **I** in which (*Si,S*)-**I** and (*Re,S*)-**I** are derived from (*S*)-**2** (Scheme 4a), while (*Si,R*)-**I** and (*Re,R*)-**I** are derived from (*R*)-**2** (Scheme 4b). The structure used to model intermediates **I** was built by ChemBio 3D Ultra 11.0 software

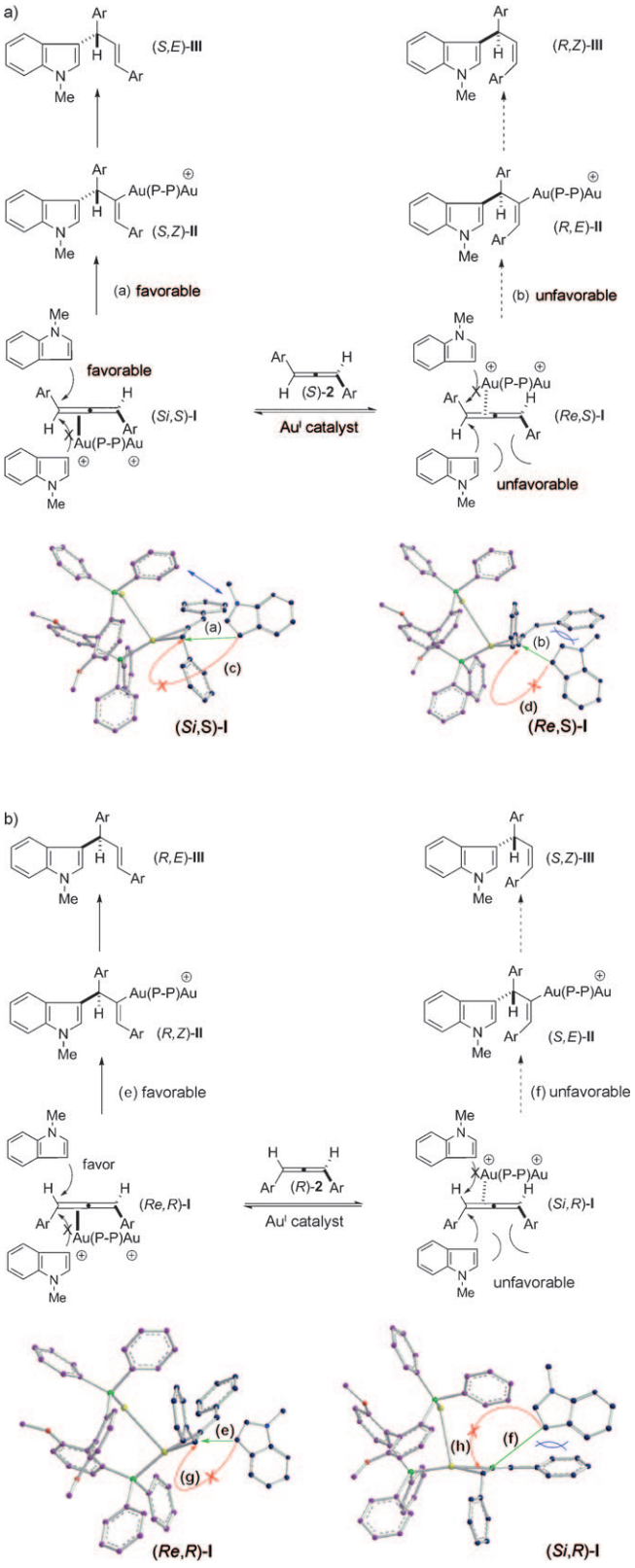

Scheme 4. Origin of the enantioselectivity.

based on the X-ray crystal structure of **4c**. As shown in Scheme 4a, the hydroarylation of (*S*)-**2** with indole would lead to products (*S,E*)-**III** and (*R,Z*)-**III** based on the established mechanism that gold-catalyzed hydrofunctionalization of allene involves outer-sphere attack of the nucleophile on a gold-allene complex from the opposite side of the gold catalyst; subsequent protonolysis of the resulting vinyl gold complex (complex (*S,Z*)-**II**, (*R,E*)-**II** in Scheme 4a; complex (*R,Z*)-**II**, (*S,E*)-**II** in Scheme 4b) could give the hydrofunctionalization product with retention of configuration of the alkene group.[3d,6f] However, only the *E* isomer was observed in our experiments. The lack of observation of the *Z* isomer can be rationalized by the unfavorable steric interaction between the indole and aryl groups of allene upon approach of indole to allene from the same side of aryl group. In this work, most of the enantiorich *E* isomers were obtained in greater than 80% product yields with greater than 30% enantioselectivities from racemic allenes. This result reveals that the catalysis involves a dynamic kinetic asymmetric transformation[6f,17] in which the chiral allenes (*S*)-**2** and (*R*)-**2** equilibrate rapidly, presumably via a zwitterionic species[10b] or a gold σ-allyl cation[10d] (Figure 10). As a consequence of the diastereomeric environment of intermediates

Figure 10. The zwitterionic species and gold σ-allyl cation.

(*Si,S*)-**I** and (*Re,R*)-**I**, one of them reacts with the indole faster than the other and is continually replenished via rapid interconversion between (*S*)-**2** and (*R*)-**2**, leading to the enantiorich product. According to the model of intermediates (*Si,S*)-**I** and (*Re,R*)-**I**, we speculate that the formation of (*S, E*)-**III** is unfavorable owing to close interaction of the ligand of the catalyst with the approaching indole unit, thereby giving the enantiorich (*R,E*)-**III**.

Effect of Intramolecular Au–Au Interaction on Enantioselectivity

The Au–Au separations of complexes **4b**,[6d] **4c**, **4d**,[13,18] **4f**, and **4h** are depicted in Table 4. As shown in Table 4, the complexes **4c** (Au-Au = 3.1473(5) Å) and **4h** (Au-Au = 2.9347(3) Å) were found to give better enantioselectivity in

Table 4. The effect of intramolecular Au–Au interaction on gold(I)-catalyzed enantioselective intermolecular hydroarylation of allenes with indoles.[a]

Complex	*d*(Au–Au) [Å]	Au–Au interaction[a]	*ee* [%]
4b	5.490	–	18
4c	3.147	+	60
4d	5.298	–	17
4f	3.786	–	6.5
4h	2.934	+	49

[a] "+" represents the presence of intramolecular aurophilic interaction; "–" indicates that no Au–Au interaction is observed.

the hydroarylation reaction than the other digold(I) complexes having no Au–Au interaction. Presumably, this is attributed to the less flexible conformation of the gold(I) catalyst constrained by the intramolecular Au–Au interaction.[18] A further comparison of the crystal structure of **4c** with that of its analogues [$(AuCl)_2$(Tol-binap)][5f] and [$(AuCl)_2$(3,5-Xylyl-binap)] **4b**[6d] reveals that [$(AuCl)_2$(Tol-binap)] and [$(AuCl)_2$(3,5-Xylyl-binap)] display intramolecular π–π stacking interactions between the two aryl groups on the phosphine ligands and this is not observed in **4c**. This π–π stacking interaction renders the structure of the binuclear gold(I) phosphine complex to be less flexible and is presumed to affect the intramolecular enantioselective hydrovinylation of allenes.[6d] In our experiments, [$(AuCl)_2$(binap)] **4a** and [$(AuCl)_2$(3,5-Xylyl-binap)] **4b** were found to lead to a lower enantioselectivity than **4c**, revealing that Au–Au interaction is probably more beneficial for the enantioinduction in our reaction than intramolecular π–π stacking interactions. Complex **4f**, an analogue of **4c**, with an intramolecular Au–Au separation of 3.786 Å, which is slightly longer than that of **4c**, led to much lower enantioselectivity than **4c**. This result further manifests that Au–Au interaction may have an instrumental effect on the enantioselective intermolecular hydroarylation. Interestingly, for **4d**, which was previously reported to efficiently catalyze intramolecular enantioselective transformation of allenes, neither Au–Au contact nor π–π stacking interaction has been observed.[13,18] The flexibility owing to the lack of Au–Au contact and π–π stacking interaction may be the reason accounting for the low enantioselectivity found for our reaction catalyzed by **4d**. As shown in the model of intermediates (*Si,S*)-**I** and (*Re,R*)-**I**, the intramolecular Au–Au interaction may pull the aryl groups on the phosphine ligands close to the reaction center, thereby facilitating enantiodiscrimination. This may account for the better enantioselectivity achieved for the reaction catalyzed by complex **4c**.

Conclusion

In summary, we have developed an enantioselective intermolecular hydroarylation of racemic allenes with indoles using a 1:2 mixture of (*S*)-(−)-MeO-biphep$(AuCl)_2$ **4c** and AgOTf as catalyst. The reaction took place under mild conditions and gave high product yields with moderate enantioselectivities. DFT calculations revealed that the reaction mechanism involving intermolecular nucleophilic addition of free indole to gold-activated allene is more likely than intramolecular cyclization via a diaurated intermediate with dual activation of allene and indole.

Experimental Section

General: All manipulations with air-sensitive reagents were carried out under a dry nitrogen atmosphere. NMR spectra were recorded on a Bruker AMX 300/400 MHz spectrometer for ^{1}H NMR and 75/100 MHz for ^{13}C NMR in $CDCl_3$. The chemical shifts are expressed in ppm and coupling constants are given in Hz. Data for ^{1}H NMR spectra are recorded as follows: chemical shift (ppm), multiplicity (s, singlet; d, doublet; t, triplet; m, multiplet), coupling constant (Hz), integration. Data for ^{13}C NMR are reported in terms of chemical shift (δ, ppm). Lower-resolution mass spectra or high-resolution mass spectra (HRMS) were obtained on a Finnigan GC-MS 4021 or a Finnigan MAT-8430 instrument using the electron impact ionization technique (70 eV).

General procedure for the synthesis of $(AuCl)_2$(L) complexes: Chiral gold complexes were synthesized according to the procedures reported in the literature.[5g] $KAuCl_4$ (0.5 mmol) was dissolved in water (5 mL), and the orange solution was placed in an ice bath. To this solution was added dropwise (ca. 35 min) tetrahydrothiophene (1.5 mmol). After stirring for 0.5 h, the pale-white solid was filtrated off, washed with water and diethyl ether, and dried under vacuum. The resulting chloro(tetrahydrothiophene)gold(I) complex was used for the next step without further purification. Then, to a solution of chloro(tetrahydrothiophene)gold(I) (1.0 mmol) in CH_2Cl_2 (5 mL) was added dropwise a solution of the phosphine ligand **L** (0.5 mmol) in CH_2Cl_2 (3 mL) for 10 min with stirring. After stirring overnight, the solvent was removed to give the $(AuCl)_2$(**L**) complex as a white solid in over 90% yield. The spectral data of the known compounds **4a–f** obtained in this work matched those data reported in the literature.[3c,5e–g,6a]

(1*R*,1′*R*,2*S*,2′*S*)-duanphos$(AuCl)_2$ (4g): Obtained as a white solid. ^{1}H NMR (400 MHz, $CDCl_3$): $\delta = 0.91$ (s, 9H), 0.96 (s, 9H), 3.24–3.31 (m, 2H), 4.25 (d, $J = 20.8$ Hz, 2H), 4.25 (d, $J = 18.8$ Hz, 2H), 7.31–7.43 ppm (m, 8H); ^{13}C NMR (75 MHz, $CDCl_3$): $\delta = 26.49$, 30.68, 30.92, 31.15, 47.92, 48.15, 48.39, 126.18, 127.74, 128.18, 129.38, 139.55, 139.95 ppm; ^{31}P NMR (160 MHz, $CDCl_3$): $\delta = 47.78$ ppm; HRMS (EI) for $[C_{24}H_{32}Au_2ClP_2]^+$ ($[M-Cl]^+$), calcd 811.0999, found 811.0986.

(+)-1,2-Bis[(2*R*,5*R*)-2,5-diisopropylphospholano]benzene$(AuCl)_2$ (4h): Obtained as a white solid. ^{1}H NMR (400 MHz, $CDCl_3$): $\delta = 0.45$ (d, $J = 6.6$ Hz, 6H), 0.78 (d, $J = 6.6$ Hz, 6H), 0.97 (d, $J = 6.6$ Hz, 6H), 1.11 (d, $J = 6.6$ Hz, 6H), 1.55–1.61 (m, 2H), 1.78–1.82 (m, 2H), 2.20–2.29 (m, 8H), 2.55–2.59 (m, 2H), 3.39–3.45 (m, 2H), 7.57–7.59 (m, 2H), 7.84–7.90 ppm (m, 2H); ^{13}C NMR (75 MHz, $CDCl_3$): $\delta = 18.43$, 21.84, 21.93, 22.01, 23.77, 23.84, 23.92, 24.26, 25.16, 27.95, 30.05, 30.16, 30.33, 34.83, 48.84, 49.07, 49.28, 50.60, 50.81, 51.03, 130.88, 136.09, 136.18, 136.27 ppm; ^{31}P NMR (160 MHz, $CDCl_3$): $\delta = 37.47$ ppm; HRMS (EI) for $[C_{26}H_{44}Au_2ClP_2]^+$ ($[M-Cl]^+$), calcd 847.1938, found 847.1926.

General procedure for the synthesis of racemic allenes 2:[9] A mixture of $KAuCl_4$ (0.02 mmol), aldehyde (2.0 mmol), piperidine (2.2 mmol), and alkyne (3.0 mmol) in water (1 mL) was stirred at 40 °C for 24 h in the absence of light under N_2 atmosphere. After the reaction, the mixture was diluted with diethyl ether or CH_2Cl_2 (10 mL) and washed successively with water (2×5 mL) and brine (5 mL), and then dried over anhydrous sodium sulfate. Filtration of the organic phase through a short pad of celite, evaporation of the solvent, and purification of the residue by flash column chromatography on silica gel using ethyl acetate/hexane as eluent afforded the corresponding racemic propargylamine. A mixture of the racemic propargylamine (0.2 mmol) and $KAuCl_4$ (0.02 mmol) in CH_3CN (5 mL) was stirred at 40 °C for 24 h. The solvent was removed under reduced pressure. The product was purified by flash column chromatography on silica gel using ethyl acetate/hexane as eluent.

1,3-Bis(4-*tert*-butylphenyl)propa-1,2-diene (2c): Yellow solid, yield of 52% for two steps. ^{1}H NMR (400 MHz, $CDCl_3$): $\delta = 1.29$ (s, 18H), 6.55 (s, 2H), 7.26–7.33 ppm (m, 8H); ^{13}C NMR (100 MHz, $CDCl_3$): $\delta = 31.79$, 35.06, 98.42, 110.16, 126.15, 127.17, 131.32, 150.86 ppm; IR (KBr, neat): $\tilde{\nu} = 2926$, 1936, 1706 cm^{-1}; EIMS *m*/*z* 304 (M^+); HRMS (EI) for $C_{23}H_{28}$, calcd 304.2191, found 304.2195.

1,3-Bis(4-fluorophenyl)propa-1,2-diene (2e): Yellow oil, yield of 45% for two steps. ^{1}H NMR (300 MHz, $CDCl_3$): $\delta = 6.58$ (s, 2H), 6.99–7.05 (m, 4H), 7.29–7.34 ppm (m, 4H); ^{13}C NMR (75 MHz, $CDCl_3$): $\delta = 97.69$, 115.47, 115.89, 128.41, 129.46, 163.85 ppm; IR (KBr, neat): $\tilde{\nu} = 2925$, 1938, 1710 cm^{-1}; EIMS *m*/*z* 228 (M^+); HRMS (EI) for $C_{15}H_{10}F_2$, calcd 228.0751, found 228.0756.

General procedure for gold(I)-catalyzed enantioselective intermolecular hydroarylation of allenes with indoles (Tables 2 and 3): A mixture of (*S*)-(−)-MeO-biphep$(AuCl)_2$ **4c** (2.5 mol%) and AgOTf (5% mol) in toluene

(2 mL) was stirred at room temperature for 15 min. Allene (0.3 mmol) and indole (1.5 mmol) were added successively and the mixture was stirred for 12 h to 20 h until completion of the reaction. The reaction mixture was concentrated and loaded directly onto a silica column; elution with ethyl acetate/hexane afforded the product.

1-Methyl-3-((*E*)-1,3-diphenylallyl)-1*H*-indole (3a): Yellow solid, analytical TLC (silica gel 60, 2% EtOAc in hexane), $R_f = 0.25$; ^{1}H NMR (300 MHz, $CDCl_3$): $\delta = 3.69$ (s, 3H), 5.09 (d, $J = 7.3$ Hz, 1H), 6.41 (d, $J = 15.8$ Hz, 1H), 6.68–6.75 (m, 2H), 6.99 (t, $J = 7.1$ Hz, 1H), 7.17–7.42 ppm (m, 13H); ^{13}C NMR (75 MHz, $CDCl_3$): $\delta = 32.69$, 46.16, 109.16, 118.15, 118.86, 119.94, 121.62, 126.30, 126.33, 127.12, 127.36, 128.39, 128.47, 130.42, 132.71, 137.53, 143.54 ppm; IR (KBr, neat): $\tilde{\nu} = 3058$, 3024, 2932, 1599, 1489, 1472, 1372, 1329, 1156, 968, 741, 700 cm^{-1}; EIMS m/z 323 (M^+); HRMS (EI) for $C_{24}H_2N$, calcd 323.1674, found 323.1675; 41% *ee* determined by HPLC (Chiral OD column, 2-propanol/hexane = 1:99, 0.7 mL min^{-1}, major isomer 12.47 min, minor isomer 13.86 min).

1-Methyl-3-((*E*)-1,3-di-*p*-tolylallyl)-1*H*-indole (3b): Yellow solid, analytical TLC (silica gel 60, 2% EtOAc in hexane), $R_f = 0.25$; ^{1}H NMR (300 MHz, $CDCl_3$): $\delta = 2.32$ (s, 3H), 2.33 (s, 3H), 3.67 (s, 3H), 5.05 (d, $J = 7.2$ Hz, 1H), 6.41 (d, $J = 15.8$ Hz, 1H), 6.61 (dd, $J_1 = 7.3$ Hz, $J_2 = 15.8$ Hz, 1H), 6.74 (s, 1H), 6.98 (t, $J = 7.4$ Hz, 1H), 7.07–7.12 (m, 4H), 7.16–7.30 (m, 6H), 7.42 ppm (d, $J = 7.9$ Hz, 1H); ^{13}C NMR (75 MHz, $CDCl_3$): $\delta = 21.03$, 21.11, 32.65, 45.73, 109.10, 117.38, 118.78, 119.99, 121.53, 126.18, 127.29, 128.32, 129.05, 129.11, 130.03, 131.91, 134.78, 135.72, 136.76, 137.15, 140.65 ppm; IR (KBr, neat): $\tilde{\nu} = 3057$, 3025, 2930, 1600, 1459, 1360, 1266, 1185, 969, 741, 701 cm^{-1}; EIMS m/z 351 (M^+); HRMS (EI) for $C_{26}H_{25}N$, calcd 351.1987, found 351.1988; 60% *ee* determined by HPLC (Chiral OD column, 2-propanol/hexane = 1:99, 0.7 mL min^{-1}, major isomer 14.76 min, minor isomer 17.56 min).

3-((*E*)-1,3-Bis(4-*tert*-butylphenyl)allyl)-1-methyl-1*H*-indole (3c): Yellow solid, analytical TLC (silica gel 60, 2% EtOAc in hexane), $R_f = 0.30$; ^{1}H NMR (300 MHz, $CDCl_3$): $\delta = 1.30$ (s, 9H), 1.34 (s, 9H), 3.68 (s, 3H), 5.06 (d, $J = 7.2$ Hz, 1H), 6.40 (d, $J = 15.8$ Hz, 1H), 6.63–6.72 (m, 2H), 6.99 (t, $J = 7.3$ Hz, 1H), 7.17–7.33 (m, 10H), 7.46 ppm (d, $J = 7.9$ Hz, 1H); ^{13}C NMR (75 MHz, $CDCl_3$): $\delta = 26.69$, 31.29, 31.41, 32.67, 45.63, 109.09, 117.25, 118.75, 120.06, 121.51, 124.85, 125.22, 125.34, 125.98, 127.32, 128.00, 129.85, 132.16, 134.84, 137.35, 140.58, 158.12, 159.23 ppm; IR (KBr, neat): $\tilde{\nu} = 3058$, 3026, 2935, 1602, 1458, 1362, 1265, 1183, 965, 741, 702 cm^{-1}; EIMS m/z 435 (M^+); HRMS (EI) for $C_{32}H_{37}N$, calcd 435.2926, found 435.2928; 56% *ee* determined by HPLC (Chiral OD column, 2-propanol/hexane = 0.6:99.4, 0.4 mL min^{-1}, major isomer 26.12 min, minor isomer 24.84 min).

3-((*E*)-1,3-Bis(4-methoxyphenyl)allyl)-1-methyl-1*H*-indole (3d): Yellow solid, analytical TLC (silica gel 60, 5% EtOAc in hexane), $R_f = 0.45$; ^{1}H NMR (300 MHz, $CDCl_3$): $\delta = 3.72$ (s, 3H), 3.78 (s, 3H), 5.02 (d, $J = 7.2$ Hz, 1H), 6.32 (d, $J = 15.8$ Hz, 1H), 6.47 (dd, $J_1 = 7.2$ Hz, $J_2 = 15.8$ Hz, 1H), 6.73 (s, 1H), 6.80–6.86 (m, 4H), 7.00 (t, $J = 7.1$ Hz, 1H), 7.16–7.31 (m, 6H), 7.39 ppm (d, $J = 7.9$ Hz, 1H); ^{13}C NMR (75 MHz, $CDCl_3$): $\delta = 32.67$, 45.29, 55.25, 55.29, 109.13, 113.75, 113.88, 117.62, 118.16, 118.80, 120.03, 121.56, 127.29, 127.39, 129.39, 129.52, 130.42, 130.92, 135.92, 158.08, 158.85 ppm; IR (KBr, neat): $\tilde{\nu} = 3058$, 3022, 2932, 1598, 1456, 1360, 1262, 1180, 962, 741, 701 cm^{-1}; EIMS m/z 383 (M^+); HRMS (EI) for $C_{26}H_{25}NO_2$, calcd 383.1885, found 383.1882; 53% *ee* determined by HPLC (Chiral OD column, 2-propanol/hexane = 3:97, 1 mL min^{-1}, major isomer 10.90 min, minor isomer 12.05 min).

3-((*E*)-1,3-Bis(4-fluorophenyl)allyl)-1-methyl-1*H*-indole (3e): Yellow solid, analytical TLC (silica gel 60, 5% EtOAc in hexane), $R_f = 0.51$; ^{1}H NMR (400 MHz, $CDCl_3$): $\delta = 3.74$ (s, 3H), 5.06 (d, $J = 7.3$ Hz, 1H), 6.32 (d, $J = 15.8$ Hz, 1H), 6.55 (dd, $J_1 = 7.3$ Hz, $J_2 = 15.8$ Hz, 1H), 6.73 (s, 1H), 6.93–7.02 (m, 5H), 7.17 (t, $J = 7.2$ Hz, 1H), 7.24–7.32 (m, 5H), 7.35 ppm (d, $J = 7.9$ Hz, 1H); ^{13}C NMR (75 MHz, $CDCl_3$): $\delta = 32.71$, 45.31, 109.27, 115.03, 115.21, 115.31, 115.50, 116.79, 118.98, 119.79, 121.76, 126.99, 127.27, 127.69, 127.79, 129.78, 129.88, 130.20, 133.47, 137.44, 139.09, 163.15, 163.75 ppm; IR (KBr, neat): $\tilde{\nu} = 3056$, 3025, 2931, 1595, 1452, 1365, 1265, 1182, 961, 741, 700 cm^{-1}; EIMS m/z 359 (M^+); HRMS (EI) for $C_{24}H_{19}F_2N$, calcd 359.1486, found 359.1485; 63% *ee* determined by HPLC (Chiral OD-H column, 2-propanol/hexane = 1:99, 0.5 mL min^{-1}, major isomer 31.62 min, minor isomer 29.41 min).

1-Methyl-3-((*E*)-1,3-di-*o*-tolylallyl)-1*H*-indole (3f): Yellow solid, analytical TLC (silica gel 60, 5% EtOAc in hexane), $R_f = 0.51$; ^{1}H NMR (300 MHz, $CDCl_3$): $\delta = 2.30$ (s, 3H), 2.41 (s, 3H), 3.72 (s, 3H), 5.29 (d, $J = 7.2$ Hz, 1H), 6.47–6.61 (m, 2H), 6.65 (s, 1H), 7.00 (t, $J = 7.2$ Hz, 1H), 7.11–7.21 (m, 6H), 7.23–7.32 (m, 3H), 7.41 (d, $J = 8.2$ Hz, 1H), 7.48–7.60 ppm (m, 1H); ^{13}C NMR (100 MHz, $CDCl_3$): $\delta = 20.09$, 20.25, 42.87, 109.62, 117.32, 119.28, 120.36, 122.07, 126.23, 126.46, 126.50, 126.76, 127.50, 127.89, 128.12, 128.66, 129.06, 130.61, 130.87, 134.06, 135.76, 136.60, 137.35, 137.91, 142.10 ppm; IR (KBr, neat): $\tilde{\nu} = 3058$, 3025, 2930, 1602, 1459, 1360, 1266, 1186, 967, 741, 701 cm^{-1}; EIMS m/z 351 (M^+); HRMS (EI) for $C_{26}H_{25}N$, calcd 351.1987, found 351.1989; 7% *ee* determined by HPLC (Chiral OD column, 2-propanol/hexane = 0.6:99.4, 0.45 mL min^{-1}, major isomer 22.17 min, minor isomer 15.07 min).

5-Chloro-1-methyl-3-((*E*)-1,3-di-*p*-tolylallyl)-1*H*-indole (3g): Yellow solid, analytical TLC (silica gel 60, 5% EtOAc in hexane), $R_f = 0.51$; ^{1}H NMR (300 MHz, $CDCl_3$): $\delta = 2.31$ (s, 3H), 2.34 (s, 3H), 3.71 (s, 3H), 4.98 (d, $J = 7.2$ Hz, 1H), 6.34 (d, $J = 15.8$ Hz, 1H), 6.56 (dd, $J_1 = 7.2$ Hz, $J_2 = 15.8$ Hz, 1H), 6.76 (s, 1H), 7.07–7.12 (m, 5H), 7.17–7.20 (m, 3H), 7.24–7.25 (m, 2H), 7.49 ppm (s, 1H); ^{13}C NMR (75 MHz, $CDCl_3$): $\delta = 21.03$, 21.13, 32.86, 45.46, 110.18, 117.18, 119.27, 121.89, 124.68, 126.19, 128.23, 128.59, 129.16, 130.29, 131.44, 134.63, 135.80, 135.94, 136.93, 140.19 ppm; IR (KBr, neat): $\tilde{\nu} = 3057$, 3025, 2932, 1697, 1597, 1504, 1227, 1158, 972, 833, 741 cm^{-1}; EIMS m/z 312 (M^+); HRMS (EI) for $C_{22}H_{20}N_2$, calcd 312.1626, found 312.1621; 40% *ee* determined by HPLC (Chiral OD column, 2-propanol/hexane = 0.6:99.4, 0.45 mL min^{-1}, major isomer 21.41 min, minor isomer 20.47 min).

Methyl 1-methyl-3-((*E*)-1,3-di-*p*-tolylallyl)-1*H*-indole-6-carboxylate (3h): Yellow solid, analytical TLC (silica gel 60, 5% EtOAc in hexane), $R_f = 0.51$; ^{1}H NMR (300 MHz, $CDCl_3$): $\delta = 2.31$ (s, 3H), 2.33 (s, 3H), 3.79 (s, 3H), 3.94 (s, 3H), 5.04 (d, $J = 6.1$ Hz, 1H), 6.35 (d, $J = 15.8$ Hz, 1H), 6.58 (dd, $J_1 = 7.2$ Hz, $J_2 = 15.8$ Hz, 1H), 6.89 (s, 1H), 7.07–7.13 (m, 4H), 7.18–7.26 (m, 4H), 7.40 (d, $J = 8.4$ Hz, 1H), 7.67 (dd, $J_1 = 1.1$ Hz, $J_2 = 8.4$ Hz, 1H), 8.10 ppm (s, 1H); ^{13}C NMR (75 MHz, $CDCl_3$): $\delta = 21.04$, 21.13, 32.88, 45.56, 51.90, 111.69, 117.95, 119.57, 119.89, 123.19, 126.19, 127.84, 128.26, 128.65, 129.17, 130.38, 130.66, 130.70, 131.39, 134.59, 135.97, 136.79, 136.98, 140.24, 168.25 ppm; IR (KBr, neat): $\tilde{\nu} = 3057$, 3026, 2926, 1742, 1600, 1458, 1362, 1265, 1152, 968, 741, 701 cm^{-1}; EIMS m/z 409 (M^+); HRMS (EI) for $C_{28}H_{27}NO_2$, calcd 409.2042, found 409.2040; 37% *ee* determined by HPLC (Chiral OD column, 2-propanol/hexane = 5:95, 0.7 mL min^{-1}, major isomer 33.35 min, minor isomer 25.20 min).

1,2-Dimethyl-3-((*E*)-1,3-di-*p*-tolylallyl)-1*H*-indole (3i): Yellow solid, analytical TLC (silica gel 60, 5% EtOAc in hexane), $R_f = 0.51$; ^{1}H NMR (300 MHz, $CDCl_3$): $\delta = 2.30$ (s, 6H), 2.62 (s, 3H), 3.66 (s, 3H), 5.09 (d, $J = 7.1$ Hz, 1H), 6.33 (d, $J = 15.8$ Hz, 1H), 6.75 (dd, $J_1 = 7.2$ Hz, $J_2 = 15.8$ Hz, 1H), 6.93 (t, $J = 7.3$ Hz, 1H), 7.07–7.19 (m, 5H), 7.22–7.30 (m, 6H), 7.49 ppm (d, $J = 7.6$ Hz, 1H); ^{13}C NMR (100 MHz, $CDCl_3$): $\delta = 11.28$, 24.49, 21.63, 30.04, 45.45, 109.07, 112.93, 119.23, 119.99, 120.86, 126.64, 127.48, 128.61, 129.12, 129.37, 129.63, 129.75, 130.62, 132.10, 133.83, 135.35, 135.90, 137.28, 141.21 ppm; IR (KBr, neat): $\tilde{\nu} = 3058$, 3021, 2928, 1599, 1457, 1361, 1265, 1182, 972, 741, 702 cm^{-1}; EIMS m/z 365 (M^+); HRMS (EI) for $C_{27}H_{27}N$, calcd 365.2143, found 365.2142; 41% *ee* determined by HPLC (Chiral OD column, 2-propanol/hexane = 1:99, 0.7 mL min^{-1}, major isomer 10.76 min, minor isomer 16.21 min).

1-Benzyl-3-((*E*)-1,3-di-*p*-tolylallyl)-1*H*-indole (3j): Yellow solid, analytical TLC (silica gel 60, 5% EtOAc in hexane), $R_f = 0.51$; ^{1}H NMR (400 MHz, $CDCl_3$): $\delta = 2.31$ (s, 3H), 2.32 (s, 3H), 5.06 (d, $J = 7.4$ Hz, 1H), 5.28 (s, 2H), 6.38 (d, $J = 15.8$ Hz, 1H), 6.70 (dd, $J_1 = 7.4$ Hz, $J_2 = 15.8$ Hz, 1H), 6.86 (s, 1H), 6.98 (t, $J = 7.4$ Hz, 1H), 7.07–7.14 (m, 7H), 7.21–7.30 (m, 8H), 7.42 ppm (d, $J = 7.9$ Hz, 1H); ^{13}C NMR (100 MHz, $CDCl_3$): $\delta = 21.03$, 21.11, 45.83, 50.00, 109.68, 119.07, 120.14, 121.77, 126.21, 126.58, 126.77, 127.46, 127.58, 128.34, 128.71, 129.08, 129.13, 130.15, 131.88, 134.79, 135.74, 136.82, 137.09, 137.78, 140.57 ppm; IR (KBr, neat): $\tilde{\nu} = 3058$, 3020, 2931, 1697, 1612, 1450, 1358, 1265, 1180, 972, 741, 702 cm^{-1}; EIMS m/z 427 (M^+); HRMS (EI) for $C_{33}H_{29}N$, calcd 427.2300, found 427.2301; 35% *ee* determined by HPLC (Chiral OD column, 2-propanol/hexane = 1:99, 0.7 mL min^{-1}, major isomer 26.13 min, minor isomer 20.37 min).

3-((*E*)-1,3-Bis(4-fluorophenyl)allyl)-5-chloro-1-methyl-1*H*-indole (3k): Yellow solid, analytical TLC (silica gel 60, 5% EtOAc in hexane), R_f = 0.51; ^{1}H NMR (400 MHz, $CDCl_3$): δ = 3.72 (s, 3H), 5.02 (d, J = 7.2 Hz, 1H), 6.29 (d, J = 15.8 Hz, 1H), 6.50 (dd, J_1 = 7.3 Hz, J_2 = 15.8 Hz, 1H), 6.74 (s, 1H), 6.94–7.01 (m, 4H), 7.12–7.14 (m, 1H), 7.18–7.25 (m, 3H), 7.28–7.32 ppm (m, 3H); ^{13}C NMR (75 MHz, $CDCl_3$): δ = 32.90, 45.04, 110.34, 115.16, 115.25, 115.44, 115.54, 116.32, 119.09, 122.12, 126.15, 127.83, 128.56, 129.69, 129.80, 131.77, 138.64, 139.22, 163.12, 163.58 ppm; IR (KBr, neat): $\tilde{\nu}$ = 3057, 3026, 2933, 1695, 1599, 1501, 1223, 1157, 970, 831, 741 cm^{-1}; EIMS m/z 393 (M^+); HRMS (EI) for $C_{24}H_{18}ClF_2N$, calcd 393.1096, found 393.1095; 51% *ee* determined by HPLC (Chiral OD-H column, 2-propanol/hexane = 1:99, 0.5 mL min^{-1}, major isomer 31.23 min, minor isomer 23.46 min).

3-((*E*)-1,3-Bis(4-fluorophenyl)allyl)-1,2-dimethyl-1*H*-indole (3l): Yellow solid, analytical TLC (silica gel 60, 5% EtOAc in hexane), R_f = 0.51; ^{1}H NMR (400 MHz, $CDCl_3$): δ = 2.35 (s, 3H), 3.67 (s, 3H), 5.08 (d, J = 7.2 Hz, 1H), 6.32 (d, J = 15.8 Hz, 1H), 6.66 (dd, J_1 = 7.1 Hz, J_2 = 15.8 Hz, 1H), 6.91–6.96 (m, 5H), 7.10 (t, J = 7.7 Hz, 1H), 7.24–7.32 ppm (m, 6H); ^{13}C NMR (75 MHz, $CDCl_3$): δ = 11.22, 30.08, 45.11, 109.24, 112.38, 115.32, 115.53, 115.72, 115.94, 119.42, 119.72, 121.09, 127.19, 128.15, 128.23, 129.91, 130.06, 130.14, 132.43, 133.92, 134.02, 137.33, 139.64, 163.08, 163.78 ppm; IR (KBr, neat): $\tilde{\nu}$ = 3052, 3018, 2925, 1596, 1452, 1360, 1261, 1175, 969, 741 cm^{-1}; EIMS m/z 373 (M^+); HRMS (EI) for $C_{25}H_{21}F_2N$, calcd 373.1642, found 373.1642; 45% *ee* determined by HPLC (Chiral OD-H column, 2-propanol/hexane = 0.8:99.2, 0.5 mL min^{-1}, major isomer 38.47 min, minor isomer 36.99 min).

3-((*E*)-1,3-Bis(4-fluorophenyl)allyl)-1-phenyl-1*H*-indole (3m): Yellow solid, analytical TLC (silica gel 60, 5% EtOAc in hexane), R_f = 0.51; ^{1}H NMR (400 MHz, $CDCl_3$): δ = 5.13 (d, J = 7.2 Hz, 1H), 6.39 (d, J = 15.8 Hz, 1H), 6.62 (dd, J_1 = 7.2 Hz, J_2 = 15.8 Hz, 1H), 6.95–7.10 (m, 6H), 7.21 (t, J = 7.9 Hz, 1H), 7.31–7.35 (m, 5H), 7.41 (t, J = 7.9 Hz, 1H) 7.48–7.49 (m, 4H), 7.55 ppm (d, J = 8.3 Hz, 1H); ^{13}C NMR (75 MHz, $CDCl_3$): δ = 39.71, 105.02, 109.56, 109.65, 109.77, 109.87, 113.76, 114.43, 114.47, 117.00, 118.59, 120.70, 120.71, 122.13, 122.21, 123.96, 124.11, 124.23, 124.30, 126.17, 133.35, 135.58, 163.05, 163.62 ppm; IR (KBr, neat): $\tilde{\nu}$ = 3055, 3019, 2960, 1599, 1498, 1457, 1371, 1226, 1086, 1003, 833, 741 cm^{-1}; EIMS m/z 421 (M^+); HRMS (EI) for $C_{29}H_{21}F_2N$, calcd 421.1642, found 421.1639; 43% *ee* determined by HPLC (Chiral OD-H column, 2-propanol/hexane = 1:99, 0.5 mL min^{-1}, major isomer 18.78 min, minor isomer 15.34 min).

3-((*E*)-1,3-Bis(4-fluorophenyl)allyl)-1-butyl-1*H*-indole (3n): Yellow solid, analytical TLC (silica gel 60, 5% EtOAc in hexane), R_f = 0.51; ^{1}H NMR (300 MHz, $CDCl_3$): δ = 0.90 (t, J = 7.3 Hz, 3H), 1.27–1.42 (m, 2H), 1.75–1.84 (m, 2H), 4.06 (t, J = 7.3 Hz, 2H), 5.06 (d, J = 7.1 Hz, 1H), 6.32 (d, J = 15.8 Hz, 1H), 6.56 (dd, J_1 = 7.2 Hz, J_2 = 15.8 Hz, 1H), 6.78 (s, 1H), 6.94–7.01 (m, 5H), 7.18 (t, J = 7.2 Hz, 1H), 7.29–7.36 ppm (m, 6H); ^{13}C NMR (75 MHz, $CDCl_3$): δ = 13.70, 20.23, 32.37, 45.36, 46.10, 109.47, 115.00, 115.20, 115.28, 115.49, 116.63, 118.84, 119.85, 121.56, 126.21, 127.07, 127.69, 127.80, 129.37, 129.88, 132.33, 136.75, 139.14, 163.13, 163.74 ppm; IR (KBr, neat): $\tilde{\nu}$ = 3056, 3022, 2930, 1610, 1458, 1361, 1227, 1180, 966, 741 cm^{-1}; EIMS m/z 401 (M^+); HRMS (EI) for $C_{27}H_{25}F_2N$, calcd 401.1955, found 401.1956; 47% *ee* determined by HPLC (Chiral OD-H column, 2-propanol/hexane = 1:99, 0.5 mL min^{-1}, major isomer 22.80 min, minor isomer 17.89 min).

Acknowledgements

We are thankful for the financial support of The University of Hong Kong (University Development Fund), Hong Kong Research Grant Council (PolyU 5027/09P), the Areas of Excellence Scheme established under the University Grants Committee of the Hong Kong Special Administrative Region, China (AoE/P-10/01), RGC Collaborative Research Fund (HKU1/CRF/08), and RGC grant (HKU 7007/08P). We thank Dr. Stephen Sin-Yin Chui and Dr. Nianyong Zhu for solving the X-ray crystal structures.

[1] a) G. A. Olah, R. Krishnamurti, G. K. S. Prakash, *Friedel–Crafts Alkylations in Comprehensive Organic Synthesis*, *Vol. 3* (Eds.: B. M. Trost, I. Fleming), Pergamon Press, Oxford, **1991**, pp. 293–339.

[2] a) M. Bandini, A. Eichholzer, *Angew. Chem.* **2009**, *121*, 9786–9824; *Angew. Chem. Int. Ed.* **2009**, *48*, 9608–9644; b) V. Terrasson, R. M. de Figueiredo, J. M. Campagne, *Eur. J. Org. Chem.* **2010**, *14*, 2635–2655; c) A. G. Doyle, E. N. Jacobsen, *Chem. Rev.* **2007**, *107*, 5713–5743; d) S.-L. You, Q. Cai, M. Zeng, *Chem. Soc. Rev.* **2009**, *38*, 2190–2201.

[3] a) C. Liu, C. F. Bender, X. Han, R. A. Widenhoefer, *Chem. Commun.* **2007**, 3607–3618; b) C. Liu, X. Han, X. Wang, R. A. Widenhoefer, *J. Am. Chem. Soc.* **2004**, *126*, 3700–3701; c) X. Han, R. A. Widenhoefer, *Org. Lett.* **2006**, *8*, 3801–3804; d) C. Liu, R. A. Widenhoefer, *Org. Lett.* **2007**, *9*, 1935–1938; e) H. Huang, R. Peters, *Angew. Chem.* **2009**, *121*, 612–615; *Angew. Chem. Int. Ed.* **2009**, *48*, 604–606; f) C.-M. Chao, M. R. Vitale, P. Y. Toullec, J.-P. Genêt, V. Michelet, *Chem. Eur. J.* **2009**, *15*, 1319–1323; g) M. Bandini, A. Eichholzer, *Angew. Chem.* **2009**, *121*, 9697–9701; *Angew. Chem. Int. Ed.* **2009**, *48*, 9533–9537.

[4] For reviews on gold catalysis, see: a) A. S. K. Hashmi, *Gold Bull.* **2004**, *37*, 51–65; b) A. Arcadi, S. Di Giuseppe, *Curr. Org. Chem.* **2004**, *8*, 795–812; c) A. Hoffman-Röder, N. Krause, *Org. Biomol. Chem.* **2005**, *3*, 387–391; d) A. S. K. Hashmi, *Angew. Chem.* **2005**, *117*, 7150–7154; *Angew. Chem. Int. Ed.* **2005**, *44*, 6990–6993; e) S. Ma, S. Yu, Z. Gu, *Angew. Chem.* **2006**, *118*, 206–209; *Angew. Chem. Int. Ed.* **2006**, *45*, 200–203; f) A. S. K. Hashmi, G. J. Hutchings, *Angew. Chem.* **2006**, *118*, 8064–8105; *Angew. Chem. Int. Ed.* **2006**, *45*, 7896–7936; g) D. J. Gorin, F. D. Toste, *Nature* **2007**, *446*, 395–403; h) A. Fürstner, P. W. Davies, *Angew. Chem.* **2007**, *119*, 3478–3519; *Angew. Chem. Int. Ed.* **2007**, *46*, 3410–3449; i) E. Jiménez-Núñez, A. M. Echavarren, *Chem. Commun.* **2007**, 333–346; j) A. S. K. Hashmi, *Chem. Rev.* **2007**, *107*, 3180–3211; k) A. S. K. Hashmi, *Catal. Today* **2007**, *122*, 211–214; l) D. J. Gorin, B. D. Sherry, F. D. Toste, *Chem. Rev.* **2008**, *108*, 3351–3378; m) Z. Li, C. Brouwer, C. He, *Chem. Rev.* **2008**, *108*, 3239–3265; n) A. Arcadi, *Chem. Rev.* **2008**, *108*, 3266–3325; o) E. Jiménez-Núñez, A. M. Echavarren, *Chem. Rev.* **2008**, *108*, 3326–3350; p) N. T. Patil, Y. Yamamoto, *Chem. Rev.* **2008**, *108*, 3395–3442; q) A. S. K. Hashmi, *Angew. Chem.* **2008**, *120*, 6856–6858; *Angew. Chem. Int. Ed.* **2008**, *47*, 6754–6756; r) N. Marion, S. P. Nolan, *Chem. Soc. Rev.* **2008**, *37*, 1776–1782; s) A. S. K. Hashmi, M. Rudolph, *Chem. Soc. Rev.* **2008**, *37*, 1766–1775.

[5] For reviews on gold asymmetric catalysis, see: a) N. Bongers, N. Krause, *Angew. Chem.* **2008**, *120*, 2208–2211; *Angew. Chem. Int. Ed.* **2008**, *47*, 2178–2181; b) R. A. Widenhoefer, *Chem. Eur. J.* **2008**, *14*, 5382–5391; c) S. Sengupta, X. Shi, *ChemCatChem* **2010**, *2*, 609–619; some selected examples: d) Y. Ito, M. Sawamura, T. Hayashi, *J. Am. Chem. Soc.* **1986**, *108*, 6405–6406; e) M. J. Johansson, D. J. Gorin, S. T. Staben, F. D. Toste, *J. Am. Chem. Soc.* **2005**, *127*, 18002–18003; f) M. P. Muñoz, J. Adrio, J. C. Carretero, A. M. Echavarren, *Organometallics* **2005**, *24*, 1293–1300; g) A. D. Melhado, M. Luparia, F. D. Toste, *J. Am. Chem. Soc.* **2007**, *129*, 12638–12639; h) I. D. G. Watson, S. Ritter, F. D. Toste, *J. Am. Chem. Soc.* **2009**, *131*, 2056–2057; i) M. Uemura, I. D. G. Watson, F. D. Toste, *J. Am. Chem. Soc.* **2009**, *131*, 3464–3465; j) Z. Zhang, S. D. Lee, R. A. Widenhoefer, *J. Am. Chem. Soc.* **2009**, *131*, 5372–5373.

[6] For enantioselective intramolecular functionalization or isomerization of allenes, see: a) Z. Zhang, R. A. Widenhoefer, *Angew. Chem.* **2007**, *119*, 287–289; *Angew. Chem. Int. Ed.* **2007**, *46*, 283–285; b) R. L. LaLonde, B. D. Sherry, E. J. Kang, F. D. Toste, *J. Am. Chem. Soc.* **2007**, *129*, 2452–2453; c) M. R. Luzung, P. Mauleón, F. D. Toste, *J. Am. Chem. Soc.* **2007**, *129*, 12402–12403; d) M. A. Tarselli, A. R. Chianese, S. L. Lee, M. R. Gagné, *Angew. Chem.* **2007**, *119*, 6790–6793; *Angew. Chem. Int. Ed.* **2007**, *46*, 6670–6673; e) Z. Zhang, C. F. Bender, R. A. Widenhoefer, *Org. Lett.* **2007**, *9*, 2887–2889; f) Z. Zhang, C. F. Bender, R. A. Widenhoefer, *J. Am. Chem. Soc.* **2007**, *129*, 14148–14149; g) G. L. Hamilton, E. J. Kang, M. Mba, F. D. Toste, *Science* **2007**, *317*, 496–499; h) I. Alonso, B. Trillo, F. López, S. Montserrat, G. Ujaque, L. Castedo, A. Lledós,

J. L. Mascareñas, *J. Am. Chem. Soc.* **2009**, *131*, 13020–13030; i) K. Aikawa, M. Kojima, K. Mikami, *Angew. Chem.* **2009**, *121*, 6189–6193; *Angew. Chem. Int. Ed.* **2009**, *48*, 6073–6077; j) R. L. LaLonde, Z. J. Wang, M. Mba, A. D. Lackner, F. D. Toste, *Angew. Chem.* **2010**, *122*, 608–611; *Angew. Chem. Int. Ed.* **2010**, *49*, 598–601; k) A. Z. González, F. D. Toste, *Org. Lett.* **2010**, *12*, 200–203; l) H. Teller, S. Flügge, R. Goddard, A. Fürstner, *Angew. Chem.* **2010**, *122*, 1993–1997; *Angew. Chem. Int. Ed.* **2010**, *49*, 1949–1953; m) F. Kleinbeck, F. D. Toste, *J. Am. Chem. Soc.* **2009**, *131*, 9178–9179.

[7] a) K. L. Toups, G. T. Liu, R. A. Widenhoefer, *J. Organomet. Chem.* **2009**, *694*, 571–575; b) M. A. Tarselli, A. Liu, M. R. Gagné, *Tetrahedron* **2009**, *65*, 1785–1789; c) M. C. Kimber, *Org. Lett.* **2010**, *12*, 1128–1131; d) R. Skouta, C.-J. Li, *Can. J. Chem.* **2008**, *86*, 616–620.

[8] a) C.-Y. Zhou, P. W. H. Chan, C.-M. Che, *Org. Lett.* **2006**, *8*, 325–328; b) V. K.-Y. Lo, Y. Liu, M.-K. Wong, C.-M. Che, *Org. Lett.* **2006**, *8*, 1529–1532; c) X.-Y. Liu, C.-H. Li, C.-M. Che, *Org. Lett.* **2006**, *8*, 2707–2710; d) C.-Y. Zhou, C.-M. Che, *J. Am. Chem. Soc.* **2007**, *129*, 5828–5829; e) X.-Y. Liu, P. Ding, J.-S. Huang, C.-M. Che, *Org. Lett.* **2007**, *9*, 2645–2648; f) M.-Z. Wang, M.-K. Wong, C.-M. Che, *Chem. Eur. J.* **2008**, *14*, 8353–8364; g) X.-Y. Liu, C.-M. Che, *Angew. Chem.* **2008**, *120*, 3865–3870; *Angew. Chem. Int. Ed.* **2008**, *47*, 3805–3810; h) X.-Y. Liu, C.-M. Che, *Org. Lett.* **2009**, *11*, 4204–4207.

[9] a) V. K.-Y. Lo, M.-K. Wong, C.-M. Che, *Org. Lett.* **2008**, *10*, 517–519; b) V. K.-Y. Lo, C.-Y. Zhou, M.-K. Wong, C.-M. Che, *Chem. Commun.* **2010**, *46*, 213–215.

[10] a) B. D. Sherry, F. D. Toste, *J. Am. Chem. Soc.* **2004**, *126*, 15978–15979; b) C. Deutsch, B. Gockel, A. Hoffmann-Röder, N. Krause, *Synlett* **2007**, 1790–1794; c) J. H. Lee, F. D. Toste, *Angew. Chem.* **2007**, *119*, 930–932; *Angew. Chem. Int. Ed.* **2007**, *46*, 912–914; d) Z. Zhang, R. A. Widenhoefer, *Org. Lett.* **2008**, *10*, 2079–2081.

[11] T. J. Brown, M. G. Dickens, R. A. Widenhoefer, *J. Am. Chem. Soc.* **2009**, *131*, 6350–6351.

[12] a) A. S. K. Hashmi, T. D. Ramamurthi, F. Rominger, *J. Organomet. Chem.* **2009**, *694*, 592–597; b) D. V. Partyka, M. Zeller, A. D. Hunter, T. G. Gray, *Angew. Chem.* **2006**, *118*, 8368–8371; *Angew. Chem. Int. Ed.* **2006**, *45*, 8188–8191; c) C. Croix, A. Balland-Longeau, H. Allouchi, M. Giorgi, A. Duchêne, J. Thibonnet, *J. Organomet. Chem.* **2005**, *690*, 4835–4843; d) P. Lu, T. C. Boorman, A. M. Z. Slawin, I. Larrosa, *J. Am. Chem. Soc.* **2010**, *132*, 5580–5581; e) L.-P. Liu, B. Xu, M. S. Mashuta, G. B. Hammond, *J. Am. Chem. Soc.* **2008**, *130*, 17642–17643.

[13] CCDC 791653 (**4d**), CCDC 791654 (**4f**), CCDC 791655 (**4c**) and CCDC 791656 (**4h**) contain the supplementary crystallographic data for this paper. These data can be obtained free of charge from The Cambridge Crystallographic Data Centre via www.ccdc.cam.ac.uk/data_request/cif.

[14] a) P. H.-Y. Cheong, P. Morganelli, M. R. Luzung, K. N. Houk, F. D. Toste, *J. Am. Chem. Soc.* **2008**, *130*, 4517–4526; a recent mechanistic study of Au^{I}-catalyzed intermolecular hydroamination of allenes: b) Z. J. Wang, D. Benitez, E. Tkatchouk, W. A. Goddard III, F. D. Toste, *J. Am. Chem. Soc.* **2010**, *132*, 13064–13071.

[15] D. Weber, M. A. Tarselli, M. R. Gagné, *Angew. Chem.* **2009**, *121*, 5843–5846; *Angew. Chem. Int. Ed.* **2009**, *48*, 5733–5736.

[16] G. Kovács, G. Ujaque, A. Lledós, *J. Am. Chem. Soc.* **2008**, *130*, 853–864.

[17] a) E. Vedejs, M. Jure, *Angew. Chem.* **2005**, *117*, 4040–4069; *Angew. Chem. Int. Ed.* **2005**, *44*, 3974–4001; b) H. Pellissier, *Tetrahedron* **2003**, *59*, 8291–8327; c) O. Pàmies, J.-E. Bäckvall, *Chem. Rev.* **2003**, *103*, 3247–3262.

[18] F. Liu, D. Qian, L. Li, X. Zhao, J. Zhang, *Angew. Chem.* **2010**, *122*, 6819–6822; *Angew. Chem. Int. Ed.* **2010**, *49*, 6669–6672.

Received: September 7, 2010
Published online: December 14, 2010

